

# Simulating Rhine River discharges using a land surface model

R. T. W. L. Hurkmans<sup>1</sup>, P. A. Troch<sup>2</sup>, R. Uijlenhoet<sup>1</sup> and E. J. Moors<sup>3</sup>

<sup>1</sup> Hydrology and Quantitative Water Management,  
Wageningen University, P. O. Box 46, 6700 AA, Wageningen, The Netherlands, email: [ruud.hurkmans@wur.nl](mailto:ruud.hurkmans@wur.nl)

<sup>2</sup> Department of Hydrology and Water Resources, University of Arizona,  
Tucson, AZ, U.S.A.

<sup>3</sup> Earth System Science and Climate Change, Wageningen University, P.  
O. Box 47, 6700 AA, Wageningen, The Netherlands

## 1. Introduction

The Rhine basin is a very densely populated and industrialized area in Central Europe, therefore, floods and droughts occurring in the basin can have vast consequences (Middelkoop et al., 2000; Kleinn et al., 2005). For example, the near-floods in the 1993 and 1995 caused many problems and huge damage (only in Germany about 900 million USD; see also Kleinn et al., (2005)). Also the drought period in 2003 impacted a wide range of sectors, from inland navigation to hydropower generation (Middelkoop, 2001). Under climate change the hydrological cycle is expected to intensify, causing more extreme precipitation events, and increasing temperatures (e.g., IPCC, 2007; Kwadijk, 1993). Both factors will have major impacts on hydrological regimes globally; the temperature increase will cause more precipitation to fall as rain instead of snow, and the winter snow pack will melt earlier in spring (Barnett, 2005). The Rhine basin, therefore, will shift from a combined rainfall and snow melt regime to a more rainfall domin-

ated regime, resulting in increased flood risk in winter and a higher probability of extensive droughts in summer.

To be prepared for these projected changes, a thorough understanding of the impacts of climate change to the hydrological regime is necessary. To assess these impacts, and to predict the frequency, timing and magnitude of floods and droughts, accurate streamflow simulations are crucial. Many studies, (e.g., Kleinn et al., 2005, Aerts et al, 2006), have been carried out to quantify the impact of climate change on streamflow, often using conceptual water balance models driven by climate scenarios to simulate future streamflow. Land surface models (LSMs), however, carry the potential to more accurately estimate hydrological partitioning (and thus streamflow) than water balance models, because the former solve the coupled water and energy balance and are able to exploit a larger part of the information provided by regional climate model output. Due to increased model complexity, on the other hand, they are also more difficult to parameterize. A recent model intercomparison study reported in Hurkmans et al., (2007), found an LSM (Variable Infiltration Capacity (VIC) model, version 4.0.5) to be more robust compared to a more conceptual water balance model (STREAM: Spatial Tools for River basins and Environment and Analysis of Management options; Aerts, 1999). An additional advantage of LSMs is their physical basis, where physical values can be assigned to model parameters, enabling to assess the influence of, for example, land cover changes.

One way to help relieving the impact of climate change is through changes in land use. For example, recent research by Bradshaw et al., (2007) indicated that deforestation can amplify flood risk. Therefore, it might be worthwhile investigating whether reforestation (e.g., of agricultural land), can delay the timing and decrease the magnitude of flood peaks. Embedded in the framework of the NeWater project, the VIC model is used to investigate the impact of climate change on the hydrological regime in the river Rhine, by using regional climate scenarios as meteorological input. For this study, no actual climate scenarios are available yet, but extreme values from 1000 years of resampled climate data (similar to previous work by Beersma et al. (2002) and Wojcik et al. (2000)) are used to assess the sensitivity of Rhine river discharge to extremes in atmospheric forcing. In addition, the influences of changes in land cover are evaluated by defining some, quite extreme, land use scenarios. By evaluating discharge simulations at various locations throughout the Rhine basin, corresponding to subcatchments of different sizes, we get an idea of the spatial scales at which land use changes can or cannot influence streamflow. In

areas that appear to be sensitive to land use changes, management strategies to relief peak flows and low-flow periods can make use of this.

The setup of this paper is as follows: in sections 2 and 3 a short overview is provided containing the available dataset, the study area and the VIC model, including its calibration. In section 4 construction and use of the climate and land use scenarios are discussed, whereas in section 5 some results are shown. Finally, in section 6 some conclusions are drawn and implications for water management are sketched.

## **2. Data and models**

### **2.1. The Rhine basin**

The river Rhine is a major European river. In Figure 1 its location and main tributaries are shown. It originates high up in the Swiss Alps where it is nourished by rain water and water from melting snow and glaciers. After leaving the Alps it forms one of the largest lakes of Europe, Lake Constance, also called Bodensee. Further downstream the Rhine forms the border between France and Germany and receives on its way the water of several important tributaries such as the rivers Neckar, Main and Mosel. After crossing the German-Dutch border, the Rhine bifurcates into three branches (Waal, Nederrijn/Lek and IJssel) and finally mouths in the North Sea. The Rhine has a length of 1320 km and a catchment area of 185.000 km<sup>2</sup>. Water discharge at Basel is around 1000 m<sup>3</sup>/s and at the German-Dutch border it is 2300 m<sup>3</sup>/s on average. The Rhine basin is a densely populated basin: around 50 million people live in the catchment area. Around 30 million of the inhabitants receive drinking water, which is directly or indirectly prepared from river water. It is a heavily industrialized area in which almost 2/3 of the chemical and pharmaceutical companies of the world can be found. It is also a very busy river with the largest seaport of the world (Rotterdam) and the largest inland harbor of the world (Duisburg). Based on its geographic and climatologic characteristics, the Rhine can be divided into three parts: the Alpine area (upstream of Basel), the middle mountain area (between Basel and Cologne) and the lowland area (downstream of Cologne). The Alpine area exists of roughly 16.000 km<sup>2</sup>, with maximum heights of 4000 m.a.s.l. (meters above sea level). About

400 km<sup>2</sup> are covered with glaciers. The upper stretch, from the source to the Bodensee, is called the Alpenrhein; the part between the Bodensee and Basel is called the Hochrhein. Main tributaries in this part are the Aare, Rheus and Limmat. In the middle part, maximum elevations range from more than 1000 m.a.s.l. in the south to about 600 m.a.s.l. in the north, while averages are between 200 and 400 m.a.s.l. Between Basel and Bingen, the river stretch is called the Oberrhein, while between Bingen and Cologne it is called the Mittelrhein. The main tributaries in the Oberrhein are the Neckar and Main. For the Mittelrhein these are the Lahn, Mosel and Sieg. The lowland includes extensive sedimentary areas: (fluvio)glacial deposits, loess, cover sands and fluvial deposits of the lower Rhine delta. The main tributaries are the Lippe, Ruhr and Vecht (Daamen et al., 1997; Middelkoop et al., 2001). Because the Rhine splits into three distributaries downstream of Lobith, we only consider the part upstream of Lobith. In this study, we use streamflow observations from Lobith and various tributaries; an overview of some characteristics of these tributaries and streamflow gauges is shown in Table 1 and Figure 1.

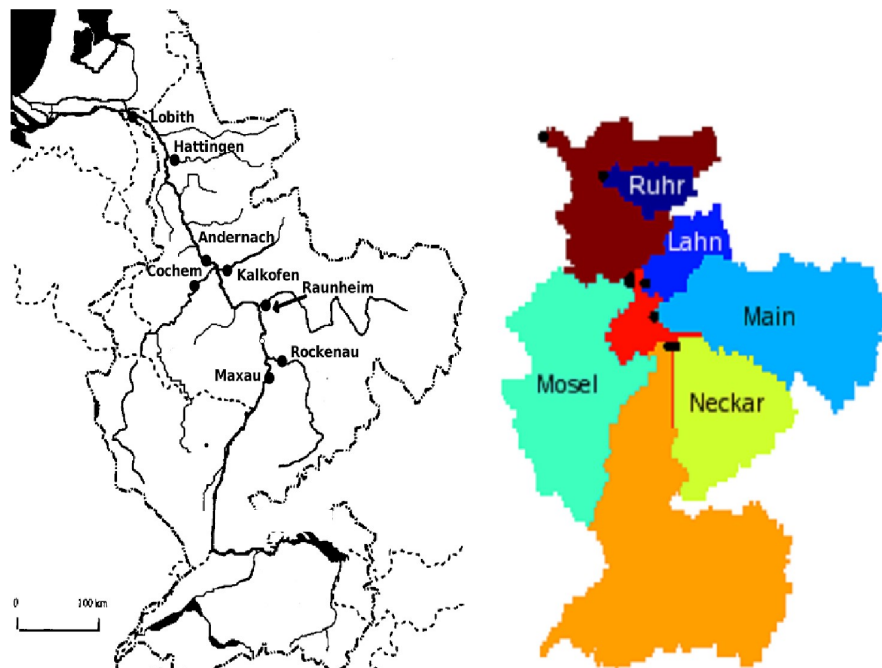


Fig 1. The Rhine basin and the locations of tributaries and gauges used in this study (left), and the discretisation used to model the various tributaries in VIC (right).

Table 1. Main tributaries of the Rhine basin and their characteristics. Mean, maximum and mean annual maximum (MAM) discharge are calculated over the period 1993-2003. Same numbers are also shown for the basin outlet Lobith.

| Tributary | Gauge     | Area<br>km <sup>2</sup> | Mean Q<br>m <sup>3</sup> /s | Max Q<br>m <sup>3</sup> /s | MAM Q<br>m <sup>3</sup> /s |
|-----------|-----------|-------------------------|-----------------------------|----------------------------|----------------------------|
| Lahn      | Kalkofen  | 5.304                   | 48                          | 587                        | 394                        |
| Main      | Raunheim  | 24.764                  | 187                         | 1991                       | 1177                       |
| Mosel     | Cochem    | 27.088                  | 364                         | 4009                       | 2650                       |
| Neckar    | Rockenau  | 12.710                  | 154                         | 2105                       | 1396                       |
| Ruhr      | Hattingen | 4.118                   | 75                          | 867                        | 611                        |
| Rhine     | Lobith    | 185.000                 | 2395                        | 11775                      | 8340                       |

## 2.2. Data

The VIC model requires data about land cover, soil type and atmospheric forcing data. Land cover data was obtained from the PELCOM project (Mücher et al., 2000); a pan-European database at a resolution of 1 km. Soil data was obtained from the global FAO dataset, described in (Reynolds et al., 2000). For atmospheric forcing data, we use a downscaled version of the ERA15 reanalysis dataset. Downscaling was carried out at the Max Planck Institut für Meteorologie using the regional climate REMO model (Jacob, 2001), in the framework of the NeWater project. The resulting dataset contains seven variables, which can all be used as input for VIC: precipitation, surface temperature, surface pressure, specific humidity, shortwave, and longwave downward radiation and wind speed, all at a spatial resolution of 0.088 degree (about 9 km) and a temporal resolution of 3 hours. The dataset spans the period from 1993 through 2003. In the remainder of this paper we will refer to this dataset as ERA15d (where stands for "downscaled"). From a comparison with observations of precipitation and temperature (for an extensive description, see Hurkmans et al. 2007), it appeared that this dataset was, in general, slightly too warm and too wet. However, the observed dataset is not suitable to force VIC (only daily precipitation and daily mean temperature) and because the climate scenarios to run later in the NeWater project are similar to the ERA15d dataset, we use the latter in the remainder of this paper as the 'reference climate'.

To represent climate variability under climate change, 1000 years of resampled data are available based on a RCM simulation from 2050-2080. With resampling we mean that individual days from the RCM simulation

were randomly (with certain constraints) ordered to create the 1000 year time series. For more detail, see for example Beersma et al. (2002) and Wojcik et al. (2002). The purpose of resampling the data is that, by extending the data over 1000 years, the probability of extreme events occurring in the dataset is much larger than in the original dataset. From these 1000 years, we selected the most extreme periods to force the VIC model and obtain the corresponding extreme discharges. More details about this process are given in section 4.

### **3. The Variable Infiltration Capacity model**

#### **3.1. Model description**

The LSM that is employed in this study, the Variable Infiltration Capacity (VIC) model (Liang et al., 1994) is a variable-layer soil-vegetation-atmosphere-transfer (SVAT) model, developed for use in general and regional circulation and weather prediction models. Its most distinguishing aspect in comparison with other LSMs is its variable infiltration capacity concept, which relates the fraction of a grid cell that is saturated and the grid cell infiltration capacity in a statistical manner. This relationship is shown graphically in the middle right plot of the VIC schematic in Figure 2. Baseflow depends non-linearly on the soil moisture content in the lowest layer, as is shown in the lower right plot of the VIC-schematic in Figure 2. Parameters defining these relationships, which control the shape of the resulting hydrograph, are typically used for calibration in previous applications of the VIC model. The sum of surface runoff and baseflow is routed along the channel network using a separate algorithm developed by (Lohmann et al., 1996), shown schematically in the right panel of Figure 2.

The model can operate in two modes: energy balance mode and water balance mode. In the energy balance mode, the coupled water and energy balances are solved to compute surface temperature, whereas in water balance mode, surface temperature is assumed equal to air temperature. In the water balance mode, the model requires less forcing data (precipitation and daily maximum and minimum temperature are sufficient) and is able to integrate at a daily time step, greatly reducing computation time. The two VIC modes are compared more extensively in (Hurkmans et al., 2007).

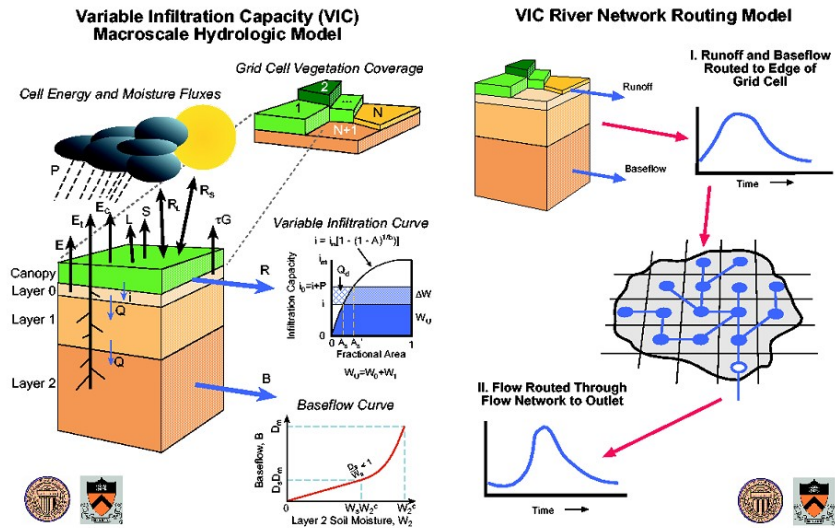


Fig 2. Schematic representation of the main features of the VIC model (left) and the routing algorithm (right). Graphs are taken from the VIC-website: <http://www.hydro.washington.edu/Lettenmaier/Models/VIC/VIChome.html>.

### 3.2. Model calibration

In previous research (Hurkmans et al., 2007), VIC was calibrated using six parameters that influence the shape of the hydrograph, controlling baseflow and surface runoff generation. These parameters were kept constant over the basin. However, it was concluded that model performance could increase when parameters are allowed to vary over the basin, because the upstream part of the basin is very different from the downstream part. We now calibrated VIC separately for each of the six subbasins described in Table 1, plus the remainder of the basin (the part around the main Rhine branch), using the same set of six parameters. Because in the water balance mode, the time step is different, a separate calibration step is required. Also this calibration was performed twice, with spatially uniform and varying parameters. For all calibration runs the ERA15d data was used for the period spanning October 1 1993 to December 31 1994. The first nine months of 1993 were used to spin up VIC. A summary of model performance indicators (Nash-Sutcliffe modeling efficiency (E; Nash and Sutcliffe,

1970), correlation coefficient (R) and relative volume error (RVE)) for all calibrations can be found in Figure 3.

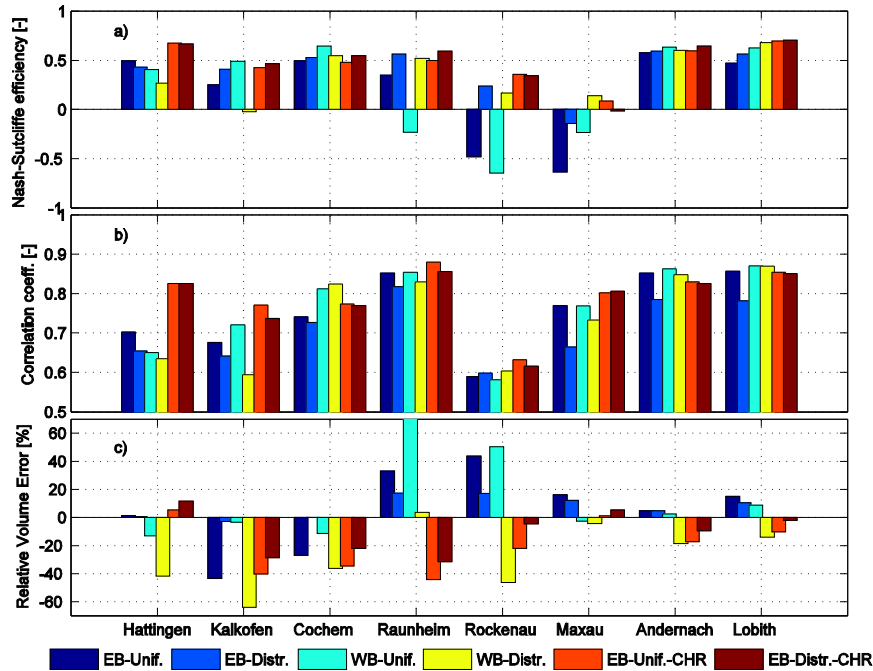


Fig 3. Histogram summarizing model performances for the calibration period. a) shows the Nash-Sutcliffe model efficiency (E), b) shows the correlation coefficient (R) and c) the Relative Volume Error (RVE). All are shown for eight gauging stations (see also Figure 1) and six different VIC simulations: both the energy balance mode (EB) and the water balance mode (WB), each calibrated uniformly and distributed. In addition, for the energy balance precipitation from the CHR dataset is used. All numbers refer to the calibration period (1/10/1993 - 31/12/1994).

As was mentioned before, the ERA15d dataset is slightly biased, causing erroneous discharges and explaining the relatively low performance indicator values in some periods. To quantify this influence, two simulations are included (uniform and distributed calibration with the energy balance mode) where ERA15d precipitation was replaced by observed precipitation. As can be seen in Figure 3, this causes overall higher model performance. Especially for Hattingen (the Ruhr), E increased significantly (almost 40 %). For some basins, especially the more Alpine ones (upstream of Maxau and the Neckar), E is often negative and all indicators are very low. This has several possible explanations: a) there are some large surface reservoirs that are not included in the model; b) the area is very mountain-

ous, with elevations up to 4000 m.a.s.l. c) snow and glacier processes add a lot of extra model complexity which is to some extent included in the model but not specifically calibrated. Especially in these subbasins, but also at Lobith and Andernach, which more or less integrate the entire basin, the water balance mode with distributed parameters appears to perform best.

## **4. Scenarios**

### **4.1. Climate scenarios**

As was explained in section 2.2., the wettest and driest period from the 1000-year resampling dataset are used to represent climate variability. In Figure 4 these two periods, each two years long since peaks often occur in winter, are shown. The period 1993-1994 from the ERA15d dataset is used as reference. In addition, in the Figure 4 all precipitation data from the observed dataset are shown to give an idea of the range of the current climate. All resampling data are spatial averages for 134 subbasins, at a daily base. Although in the future all seven variables required to force VIC will be resampled, at this moment it is only possible to use precipitation and daily maximum and minimum temperatures. This is another reason to use the VIC simulation in water balance mode with distributed parameters, which also turned out to perform best as described in the previous section.

### **4.2. Land use scenarios**

As a basis for the land use scenarios we use the PELCOM dataset (see section 2), which was also used to force VIC for the calibration runs. From this dataset we derived two scenarios: one scenario where all agricultural land (excluding grass) is changed into forest, and a second scenario where the fraction of urban area is increased arbitrarily with about 47%. To increase the fraction of urban area, existing urban areas are selected and extended, so no new urban areas are created. Urban areas were selected using a moving filter of 6 by 6 pixels (in the original 1 by 1 km PELCOM land-use map); if at least 30% of the 16 pixels in the filter window were urban, all pixels are assigned parameters were assigned the label 'urban'. Figure 5 shows maps of the main land cover classes for the reference situation and two scenarios, as well as their fractions of the total area.

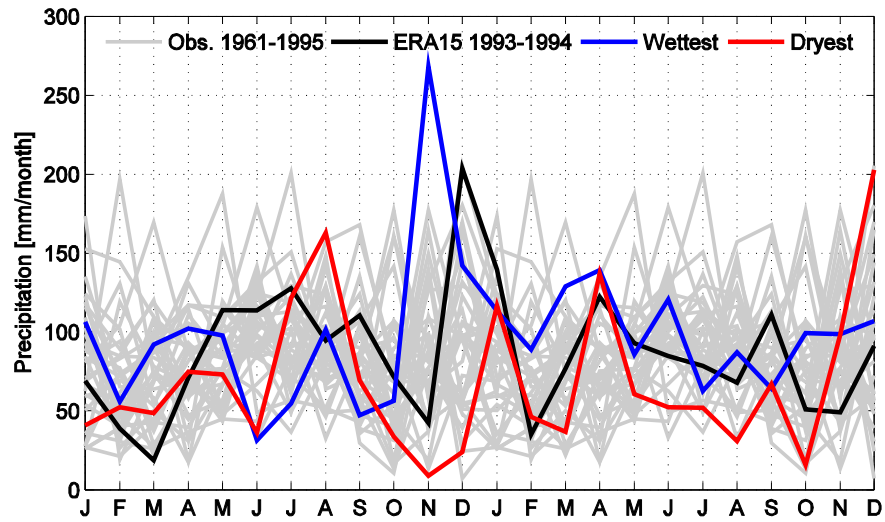


Fig 4. Precipitation from all datasets used in this paper. Gray lines reflect the years in the dataset containing observations, the black line represents years 1993-1994 from the ERA15d dataset and blue and red lines represent the most extreme years from the 1000 year of resampling data: blue is the 2-year period containing the highest 10-day precipitation, red reflects the two 2-year period containing the lowest 90-day precipitation.

We now use VIC to simulate for each of the three climates, i.e., reference (ERA15d 1993-1994), wet and dry, the three land use scenarios, i.e., reference (current), forested and urbanized, resulting in nine simulations spanning two years. Results of these simulations are shown and described in section 5.

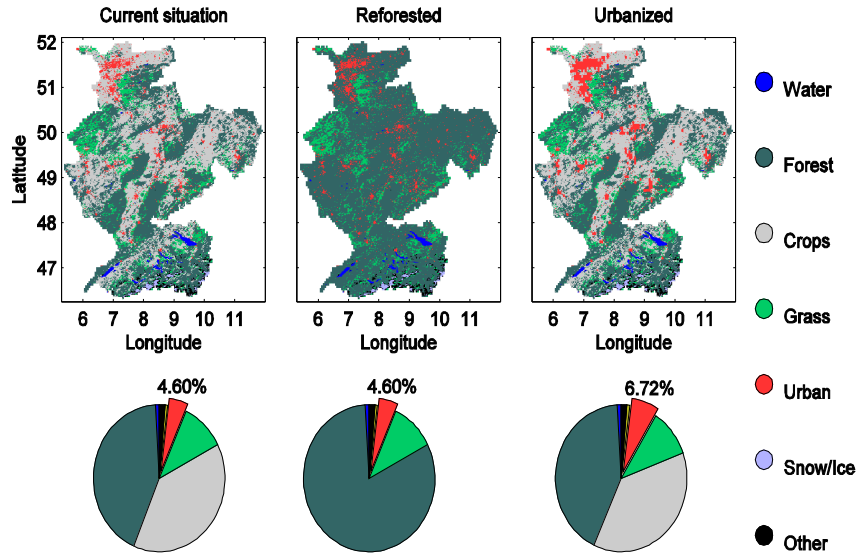


Fig. 5. Land cover scenarios used in this paper: the current situation (left), a scenario where all agricultural land is forested (middle), and a scenario with a significant increase (47 %) of urban area (right). The maps show the spatial distribution of the main land use types over the Rhine basin, the pie charts show their relative importance.

## 5. Results

### 5.1. Flood peaks

As was explained in section 4, nine VIC simulations were carried out, all spanning two years. We use three climatic scenarios, wet, reference en dry, and three land use scenarios: current, forested and urbanized. First, the wet climate scenario is discussed, with an emphasis on flood peaks. Figure 6 shows the 100 day window centered on the largest peak in a) the ERA15d reference simulation (the near-flood in 1993) and b) the wettest 2-year period from the resampling data (see Figure 4). All results are shown at eight locations in the Rhine basin for the three land use scenarios.

In addition, Table 2 shows the magnitude and timing of the flood peaks depicted in Figure 6. With timing, the shift in time of the flood peak caused by the land use change with respect to the current situation is meant. As is shown in Figure 6, the overall influence of land use changes is very small. Only for the Lahn basin (gauge Kalkofen) a significant difference can be seen. Here, the main peak from the reference climate (1993) is diminished so much by forestation that it is not the highest peak in the displayed window anymore (hence the 34 day shift in timing in Table 2). For the extreme peak in the resampling data, the influence of land use change seems much less, but by forestation the peak is still diminished by some 8% (Table 2). What is striking is that forestation does not always diminish the magnitude of flood peaks: for the area upstream of Maxau, and to lesser degree also the Mosel area, peaks are slightly amplified: by 7% for the ERA15d peak at Maxau. Since the bulk of the discharge that passes Lobith originates upstream of Maxau, this amplification is propagated to the gauges at Andernach and Lobith, resulting at an increased discharge at Lobith of about 5 percent for the peak in the resampling period and 3 percent for the 1993 peak. What causes the amplification of the flood peak is not clear, more research is needed to investigate the exact model parameterization for each land use type in VIC.

The increased portion of urban area does not appear to have any influence at all. Overall, peaks are increased slightly but not significantly. For the areas that were not densely populated in the first place, such as upstream of Maxau, there is no change at all. The most densely populated area is close to the basin outlet; therefore, this area is only represented in the values for Lobith. Indeed, the increase in magnitude at Lobith caused by urbanization is with about 2% larger than for the tributaries, especially in absolute values (about  $130 \text{ m}^3/\text{s}$ ). This is more than would be expected from the tributaries, especially since at some tributaries (Ruhr, Main) the values actually decrease. This decrease is very small, however, we can give no satisfying explanation for this feature at the moment.

The difference in magnitude between the two flood peaks is, when seen over the entire basin (at Lobith), surprisingly small. In some parts of the basin, the peak in the resampling dataset is more than double the peak in 1993, while for some other tributaries the opposite is true. Apparently there was a strong spatial variability in the rainfall over the basin.

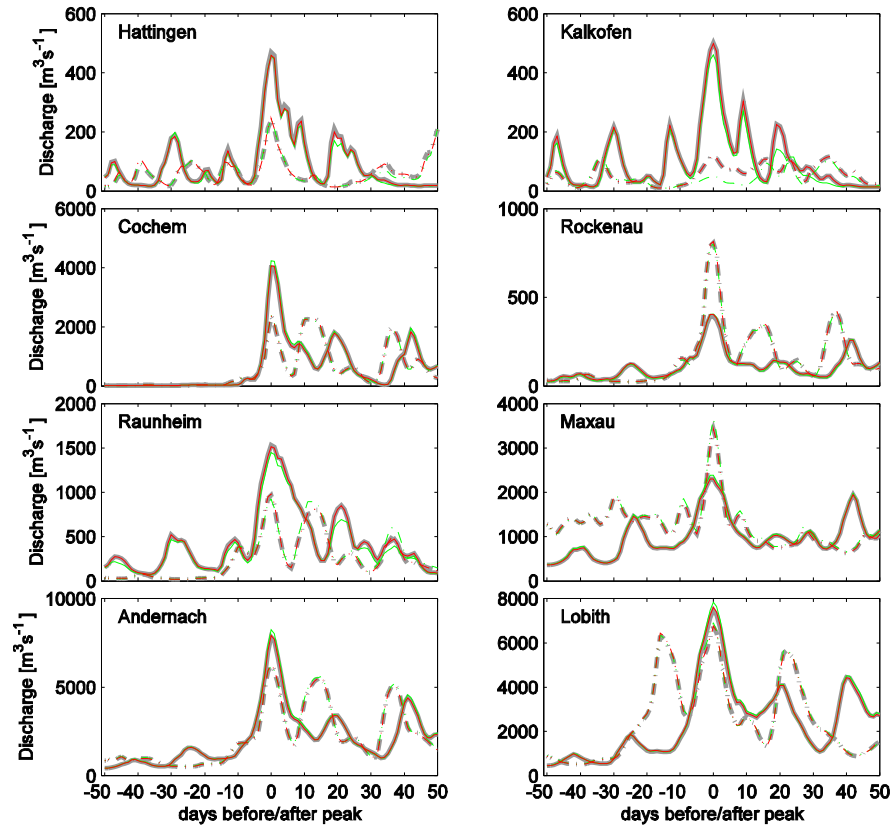


Fig. 6. Time series of discharge centered around the largest peak in the ERA15 reference period (1993; dashed lines) and the peak following from the largest 10-day precipitation amount encountered in the resampling dataset (solid lines). A window of 50 days before and after the peaks is used. For each of the extreme events, 3 land use scenarios are plotted (Figure 5): current (gray), forested (green) and urbanized (red). All is shown for eight streamflow gauges representing sub-basins of varying size (see Table 1).

Tab. 2. Magnitude and timing of peak flows of six VIC simulations: the current (ERA15d) and wet climate scenario, and the current (C), forested (F) and urbanized (U) land use scenario, for all eight gauging stations. Values for timing represent shifts in days compared to the C land use scenario. Positive values indicate delay of the peak.

| Stations  | Magnitude [ $\text{m}^3\text{s}^{-1}$ ] |      |      |            |      |      | Timing [days] |   |            |   |
|-----------|---|------|------|------------|------|------|---------------|---|------------|---|
|           | ERA15d                                  |      |      | Resampling |      |      | ERA15d        |   | Resampling |   |
|           | C                                       | F    | U    | C          | F    | U    | F             | U | F          | U |
| Hattingen | 243                                     | 245  | 245  | 470        | 458  | 459  | 0             | 0 | 0          | 0 |
| Kalkofen  | 118                                     | 119  | 119  | 502        | 462  | 498  | -34           | 0 | 0          | 0 |
| Cochem    | 2359                                    | 2400 | 2385 | 4018       | 4228 | 4062 | 0             | 0 | 0          | 0 |
| Rockenau  | 806                                     | 799  | 814  | 392        | 405  | 404  | 0             | 0 | 0          | 0 |
| Raunheim  | 965                                     | 919  | 990  | 1529       | 1446 | 1515 | 0             | 0 | 0          | 0 |
| Maxau     | 3427                                    | 3648 | 3427 | 2295       | 2384 | 2297 | 0             | 0 | -1         | 0 |
| Andernach | 6240                                    | 6235 | 6282 | 7829       | 8237 | 7913 | 0             | 0 | 0          | 0 |
| Lobith    | 6720                                    | 6911 | 6768 | 7469       | 7832 | 7601 | 0             | 0 | 0          | 0 |

Tab. 3. Average discharge and days under a threshold for all simulations shown in Figure 7, for all 8 gauging stations. The threshold was defined as half of the long-term mean discharge (see Table 1).

| Stations  | Mean discharge [ $\text{m}^3\text{s}^{-1}$ ] |     |     |            |    |    | # days under threshold |    |    |            |    |     |
|-----------|--|-----|-----|------------|----|----|------------------------|----|----|------------|----|-----|
|           | ERA15d                                       |     |     | Resampling |    |    | ERA15d                 |    |    | Resampling |    |     |
|           | C  | F   | U   | C          | F  | U  | C                      | F  | U  | C          | F  | U   |
| Hattingen | 34   | 34  | 35  | 8          | 8  | 8  | 12                     | 12 | 11 | 18         | 18 | 181 |
| Kalkofen  | 25   | 24  | 25  | 10         | 8  | 10 | 12                     | 11 | 11 | 17         | 17 | 173 |
| Cochem    | 13   | 13  | 13  | 68         | 66 | 68 | 18                     | 18 | 18 | 15         | 15 | 156 |
| Rockenau  | 117  | 114 | 118 | 32         | 30 | 32 | 97                     | 98 | 97 | 16         | 16 | 159 |
| Raunheim  | 58   | 59  | 61  | 72         | 72 | 74 | 14                     | 14 | 14 | 14         | 14 | 143 |
| Maxau     | 869  | 900 | 869 | 50         | 52 | 50 | 11                     | 10 | 11 | 14         | 14 | 146 |
| Andernach | 101  | 103 | 101 | 68         | 69 | 68 | 11                     | 10 | 11 | 15         | 15 | 154 |
| Lobith    | 108  | 111 | 109 | 71         | 72 | 71 | 12                     | 11 | 11 | 15         | 15 | 155 |

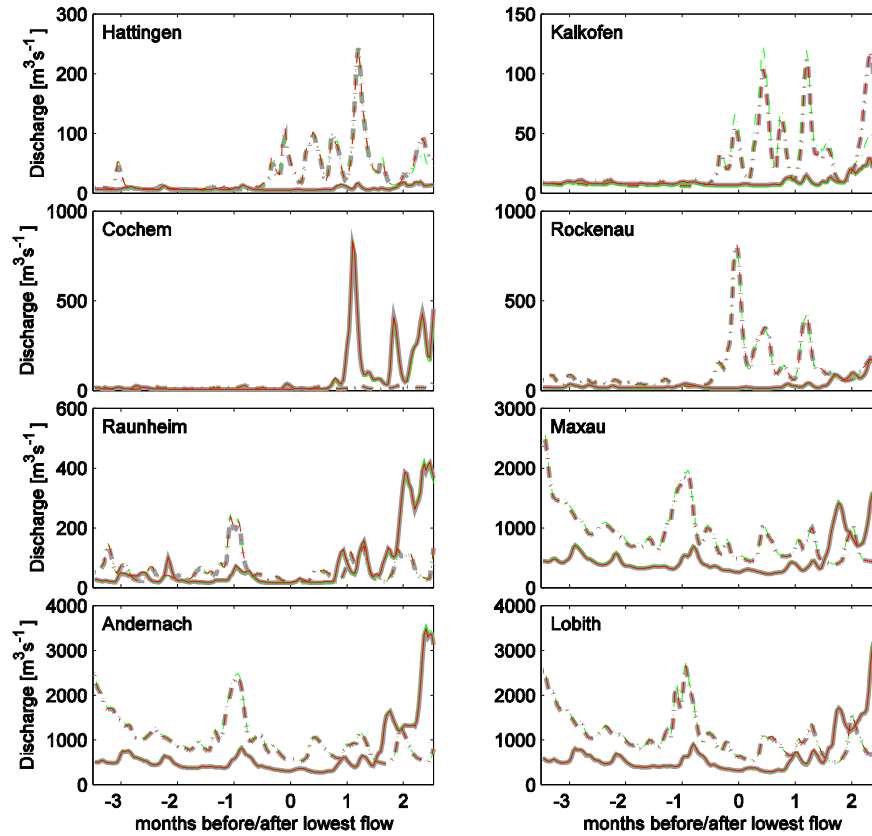


Fig 7. As Figure 6, but now the time series are centered around the lowest monthly discharge encountered in the 1993-1994 reference simulation and the simulation based on the driest 90-day period encountered in the resampling dataset. The displayed period now spans six months.

## 5.2. Low flow periods

In addition to the extreme peak events, extreme low-flow periods were investigated. Figure 7 shows a 90 day window centered around the most extreme event encountered in both the 1993-1994 reference period and the driest 2 year period from the resampling dataset (Figure 4). Again, all plots contain all three land use scenarios: current (C), forested (F) and urbanized (U). Table 3 shows the mean discharge and the number of days under a

threshold for the specified 90-day window. The threshold is defined as half the long-term mean observed discharge for the streamflow gauge under consideration. The driest period from the resampling dataset is indeed extremely dry. For example for the Ruhr, discharge never exceeds the threshold value. However, there is again a lot of spatial variability: in the Mosel area, some precipitation events occur in the resampling dataset, whereas in the ERA15d reference period, discharge never exceeds the threshold value.

Overall, the influence of land use change appeared to be smaller than in case of the peak flows. For the tributaries there is no influence at all, only for the area upstream of Maxau, there is a small (about 4%) increase in average streamflow for the forested scenario. However, at Lobith and Andernach, most of this increase is dampened by the lower Rhine basin. The part upstream of Maxau has the largest portion of forest; therefore it is not strange that only for this part an influence can be seen. Since the largest concentrations of urban areas can be found in the part close to the basin outlet (Figure 5), the influence of urbanization, if any, only shows in the number for Lobith, where it is masked by the bulk of discharge passing from the entire catchment.

## 6. Summary and conclusions

In this study, we used a state-of-art land surface model to simulate streamflow at eight locations throughout the Rhine basin. Because the model can be operated in two modes, one where both the water and energy balances are solved and one where only the water balance is solved, and different calibration setups are possible, we first compared model results for the two modes, both using either spatially constant or distributed parameters. Based on these results and data availability of climate scenario data, as well as required computation time, we chose to carry out simulations using VIC in the waterbalance mode with spatially distributed parameters. Subsequently, we used this model setup to assess the influence of climate variability and changes in land use. Apart from the reference situation, the period 1993-1994 using re-analysis data as meteorologic forcing and the current land use situation, we selected an extremely wet episode and an extremely dry episode from a 1000 year dataset of resampled regional climate model output data. To represent land use change, we selected a scenario where all crop land was forested, and one with an increase in urban area of about 47%.

For the extremely wet case, the rainfall appears to be very spatially variable, leading to major peaks in some small tributaries and hardly any rain in others. When the entire basin is considered, therefore, the increase of the discharge peak is only a modest 13%. When the extremely dry episode is considered, rainfall appeared to occur at a few tributaries. Over the 180 day period that is examined, however, mean discharge at Lobith is about 35% lower than in the reference situation. In the reference situation, we used the period 1993-1994 similar to the extremely wet case. Although the summer of 1993 was relatively dry, it would be interesting to compare the summer of 2003, which is the driest period in the ERA15d record, with the extreme from the resampling. We will incorporate this in the research in the future. Also the spatial distribution of precipitation, which showed strongly in the resulting hydrographs, will be examined in more detail.

Changes in land use appeared to have only a very minor influence on discharge. Although the forestation of all arable land is an extreme scenario, the effects are rather small. The effects are not always the same, for example after forestation the peak magnitude decreases for the Main and the Lahn, while it increases for many other parts of the Rhine, including the basin outlet. Surprisingly, forestation slightly (about 3-5%) increases the flood peak at Lobith. Urbanization has the same effect but to a much smaller degree. This is not very surprising, since in the urbanized scenario the total fraction of urban area is still only 7%. As to why forestation slightly increases the flood peak, we do not have a satisfying answer now. The actual model parameterization of the vegetation types was not changed from the default values in the model. In VIC, the main differences between forest and crop land are the higher leaf area index, rooting depth, and roughness length for forest, whereas the albedo is higher for crop land. This would lead to higher transpiration, but since most of the forest is deciduous and the peak flows occur during winter, transpiration will be very small. More research is needed to answer this question.

Concluding, it can be said that for water management purposes, land use changes upstream in the basin only have very local effects. For example, only in the relatively small Lahn basin forestation significantly changed the resulting streamflow. However, for really extreme peaks such as our peak flow scenario this influence is much smaller. In the Lahn basin, the current dominant land use type is arable land, therefore forestation has a relatively large influence. For each area, specific land use changes, depending on the current dominant cover should be designed. Therefore, more scenarios should be taken into account than the two that are studied here. When streamflow from several areas in the basin could be altered as much as for example in this study the Lahn changed by forestation, it

could impact the shape of peaks passing the basin outlet. To relief lengthy low-flow periods, however, the influence of land use changes like this seems to be too small. However this might be different for other kinds of changes than used in this study, for example, creation of wet-land-type areas.

## 7. Acknowledgments

This research was supported by the European Commission through the FP6 Integrated Project NeWater and the BSIK ACER project Climate Changes Spatial Planning Programme. We thank the following people for providing data: Daniela Jacob and Eva Mazurkewitz from the Max Planck Institut für Meteorologie, Hamburg, Germany for the atmospheric forcing data; Hendrik Buiteveld from RIZA, Arnhem, The Netherlands for stream-flow observations and Alexander Bakker from KNMI for the resampling datasets.

## 8. References

- Aerts, J.C.J.H., M. Kriek and M. Schepel, 1999, "STREAM (Spatial Tools for River Basins and Environment and Analysis of Management Options): 'Set up and requirements'", *Phys. Chem. Earth*, 24, 591-595 , S1464-1909(99)00049-0
- Aerts, J.C.J.H., H. Renssen, P.J. Ward, H. de Moel, E. Odada, L.M. Bouwer and H. Goosse, 2006, "Sensitivity of global river discharges under Holocene and future climate conditions", *Geophys. Res. Lett.*, 33, L19401, doi:10.1029/2006GL027493
- Barnett, T.P., J.C. Adam and D.P. Lettenmaier, 2005, "Potential impacts of a warming climate on water availability in snow-dominated regions", *Nature*, 438, 303-309 , doi:10.1038/nature04141
- Beersma, J.J., 2002, "Rainfall Generator for the Rhine Basin: Description of 1000-Year simulations", KNMI report nr. 186-V
- Bradshaw, C.J.A., N.S. Sodhi, K.S. Peh and B.W. Brook, 2007, "Global evidence that deforestation amplifies flood risk and severity in the developing world", *Global Change Biology*, 13 , 1-17, doi:10.1111/j.1365-2486.2007.01446.x

- Daamen, K., D. Gellens, W. Grabs, J.C.J. Kwadijk, H.Lang, H. Middelkoop, B.W.A.H. Parmet, B.S.A. Schulla and K. Wilke, 1997, "Impact of Climate Change on Hydrological Regimes and Water Resources Management in the Rhine Basin", Commission for the Hydrology of the Rhine (CHR)
- Hurkmans, R.T.W.L., H. de Moel, J.C.J.H. Aerts and P. A. Troch, 2007, "Water balance versus land surface model to simulate Rhine river discharges", *Water Resour. Res.*, in press.
- IPCC, 2007, "Fourth assessment report: Climate change 2007: Climate change impacts, adaptation and vulnerability. Summary for policy makers", *Intergovernmental Panel on Climate Change*
- Jacob, D., 2001, "A note to the simulation of the annual and inter-annual variability of the water budget over the Baltic Sea drainage basin", *Meteorol. Atmos. Phys.*, 77, 61-73
- Kleinn, J., C. Frei, J. Gurtz, D. Lüthi, P.L. Vidale and C. Schär, 2005, "Hydrologic Simulations in the Rhine Basin Driven by a Regional Climate Model", *J. Geophys. Res.*, 110 , doi:10.1029/2004JD005143
- Kwadijk, J., 1993, "The Impact of Climate Change on the Discharge of the River Rhine", *Ph.D. thesis University of Utrecht*
- Liang, X., D.P. Lettenmaier, E.F. Wood and S.J. Burges, 1994, "A simple hydrologically based model of land surface water and energy fluxes for general circulation models", *J. Geophys. Res.*, 99, 14415-14458
- Lohmann, D., R. Nolte-Holube and E. Raschke, 1996, "A large-scale horizontal routing model to be coupled to land surface parameterization schemes", *Tellus*, 48A, 708-721
- Middelkoop, H., K. Daamen, D. Gellens, W. Grabs, J. Kwadijk, H. Lang, B. Parmet, B. Schadler, J. Schulla and K. Wilke, 2001, "Impact of climate change on hydrological regimes and water resources management in the Rhine basin", *Climatic Change*, 49, 105-128
- Mücher, S., K. Steinnocher, J. Champeaux, S. Griguolo, K. Wester, C. Heunks and V. van Katwijk, 2001, "Establishment of a 1-km Pan-European Land Cover database for environmental monitoring", *ISPRS*, 33
- Nash, J.E. and I. V. Sutcliffe, 1970, "River flow forecasting through conceptual models. Part I - A discussion of principles", *J. Hydrol.*, 10, 282-290

Reynolds, C.A., T. J. Jackson and W.J. Rawls, 2000, "Estimating Water-Holding Capacities by Linking the Food and Agriculture Organization Soil Map of the World with Global Pedon Databases and Continuous Pedotransfer Functions", *Water Resour. Res.*, 36, 3653-3662

Wojcik, R., J.J. Beersma, and T.A. Buishand, 2000, "Rainfall generator for the Rhine basin: multi-site generation of weather variables for the entire drainage area", *KNMI report nr. 186-IV*